Development of the Silicon Tracker and of a YAG:Ce Calorimeter for Proton Computed Radiography

D. Menichelli[b,c], M. Bruzzi[b,c], M. Bucciolini [a,b], G. Candiano[f], G. A. P. Cirrone[f], C. Civinini[b], G. Cuttone[f], D. Lo Presti[d,e], L. Marrazzo[b,g], S. Pallotta[a,b], N. Randazzo[e], V. Sipala[d,e], C. Talamonti [a,b], M, Brianzi[b], M. Tesi[c].

a) Dipartimento di Fisiopatologia Clinica, Università degli Studi di Firenze.

b) INFN, sezione di Firenze.

c) Dipartimento di Energetica, Università degli Studi di Firenze.

d) Dipartimento di Fisica, Università degli Studi di Catania.

e) INFN, sezione di Catania.

f) Laboratori Nazionali del Sud-INFN, Catania.

g) Azienda Ospedaliero-Universitaria Careggi, Firenze.

INTRODUCTION

Main advantages of hadron-therapy with respect to conventional gamma-Xray therapy are:

i) lower dose to healthy tissues in front of the tumor;

ii) healthy tissues beyond the tumor are not damaged;

iii) Multiple scattering for protons is small enough that a very sharp dose profile can be maintained. Lateral healthy tissues are not damaged.

The stopping power distributions are the main parameters for dose calculation in hadron therapy.

They are derived from measured attenuation coefficients μ of conventional xCT

But protons and photons interact differently with matters...

... “*The error intrinsic in this conversion (due to m(he,Z) dependency on atomic number and electron density) is the principal cause of proton range indetermination (3%, up to 10 mm in the head).*”

[Schneider U. (1994), Med Phys. 22, 353]

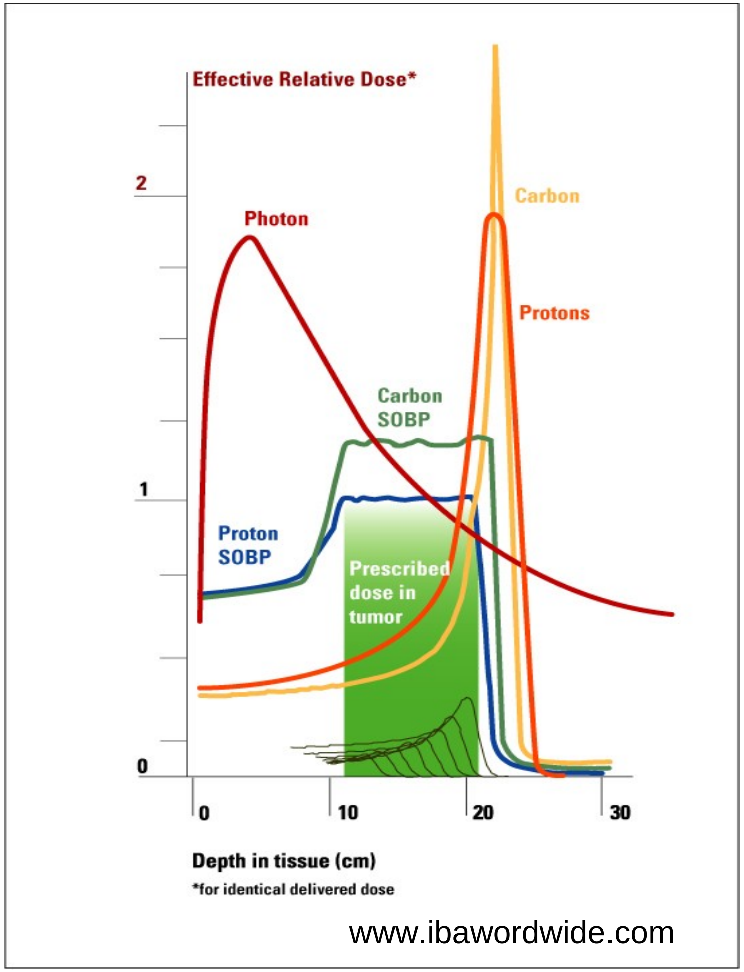

THE “PRoton IMAging PROJECT

AIMS

a) direct measurement of stopping power.
b) Precise patient positioning before every treatment.
c) Lower dose to the patient, with respect to xCT (according to MC simulations).
d) Increase of low-contrast resolution.

SPECIFICATIONS

Proton Energy	250-270 MeV
Proton rate	~10^6 1/sec
Space resolution	< 1 mm
electron density resolution	< 1%
Radiation hardness	>1000 Gy
Dose per scan	<5 cGy

PROGRAM

1) Realize a high-performance prototype for proton radiography.
2) Develop suitable imaging algorithms:
   - -analysis of old data;
   - -MC simulations.
3) Pre-clinical validation of the prototype.
4) Conceive a configuration for a pCT system:
   - -hardware and data acquisition;
   - -reconstruction algorithms (ART, SART...).

A research supported by:

INFN (PRIMA & PRIMA+ Experiments);

MIUR (PRIN2006 funding).

BACKGROUND

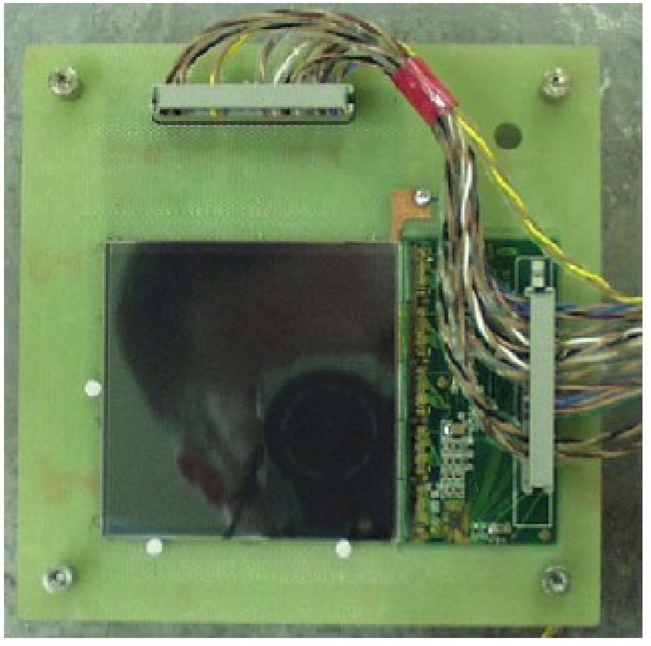

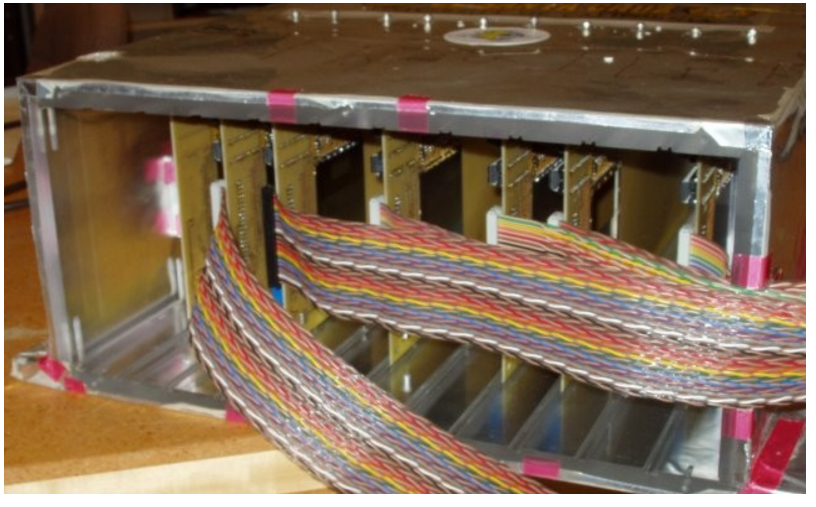

Initial studies with a Si single-sided strip telescope by UCSC and LLUMC.

Use of Si detectors (194 µm pitch, 400 µm thickness) to measure:
a) protons trajectory;
b) energy loss, from time over threshold (TOT).

Limits:
1) slow acquisiton rate (1kHz).
2) Low energy resolution (25% at 250 MeV), improved in a later prototype by a separate calorimeter.

H. F. -W. Sadrozinski et al., NIM A 514 (2003) 215–223.
M. Bruzzi et al. , IEEE Trans. Nucl. Sci., 54 (2007) 140 - 145.

MAIN DIFFICULTY WITH pCT: multiple Coulomb scattering

A possible solution:

1. single proton tracking.
2. Determination of protons Most Likely Path (MLP).

Entrance and exit angles and positions are boundary conditions for MLP Calculation.

$$-\frac{dE}{dx}(\mathbf{r}) = \eta_e(\mathbf{r}) F(I(\mathbf{r}), E(\mathbf{r}))$$

$$\eta_e = N_A Z \rho / A$$

$$-\int_{E_{in}}^{E_{out}} \frac{dE}{F(I_{water}, E)} = \int_L \eta_e(\mathbf{r}) dl$$

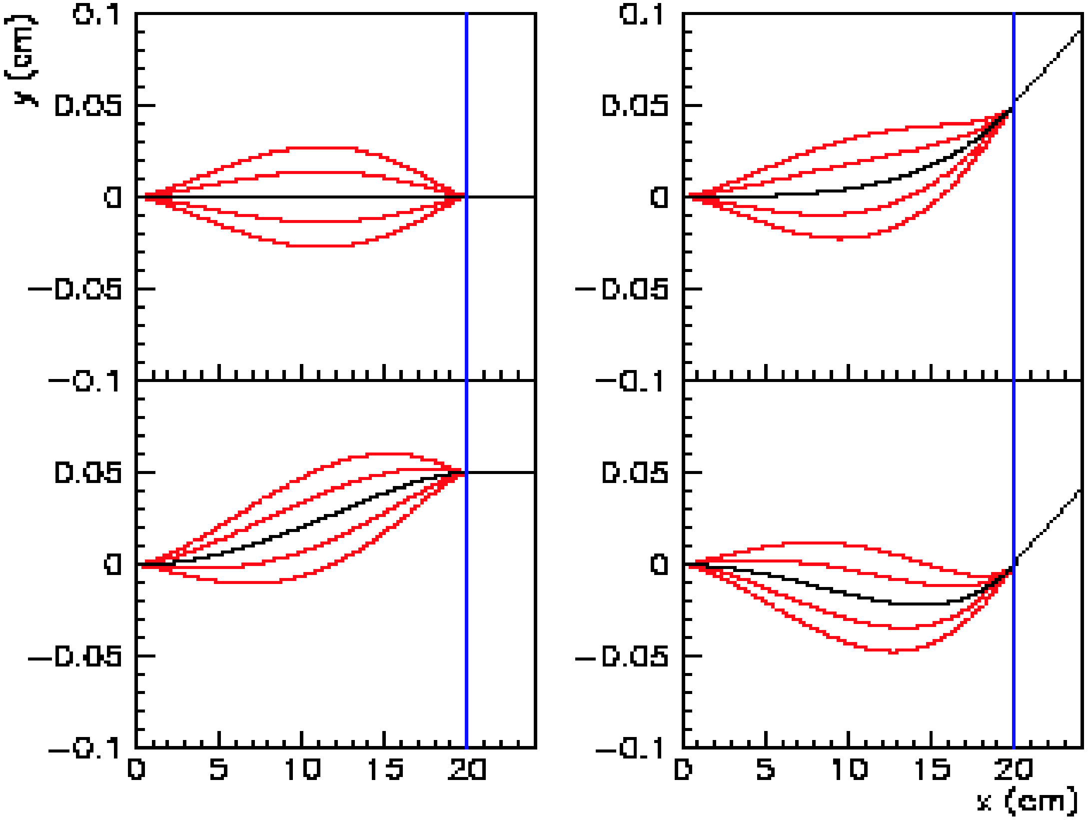

200 MeV Protons, 20 cm water
Most Likely, 1σ and 2σ path
D C Williams Phys. Med. Biol. 49 (2004) 2899–2911

CONCEPT

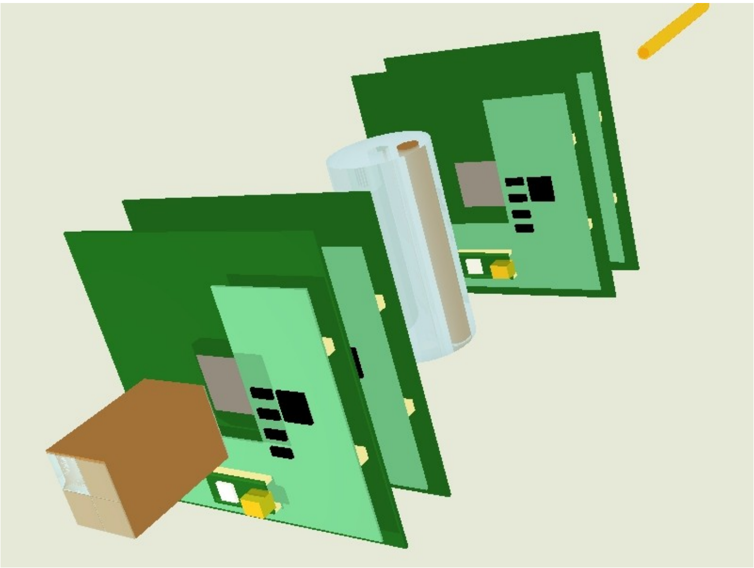

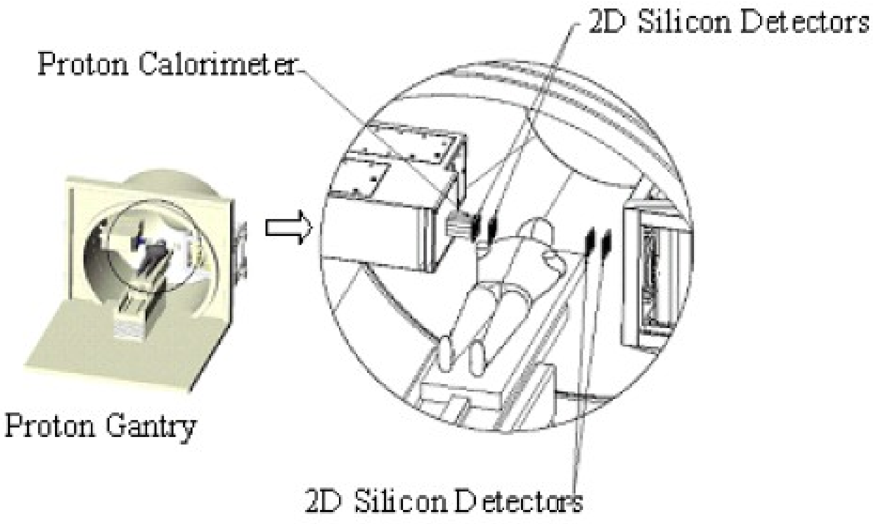

Step 1: proton Computed Radiography
(fixed hardware, fixed phantom).

Step 2: proton Computed Tomography
(fixed hardware, rotating phantom).

Step 3: "full" proton Computed Tomography
(with a rotating gantry).

The beam used for the treatment is employed (selecting a kinetic energy high enough) also for pCT

ARCHITECTURE

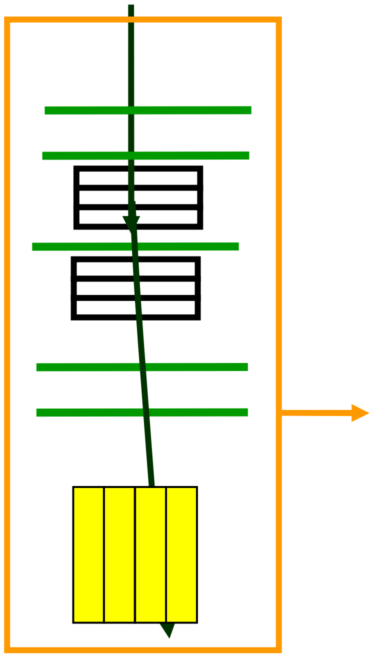

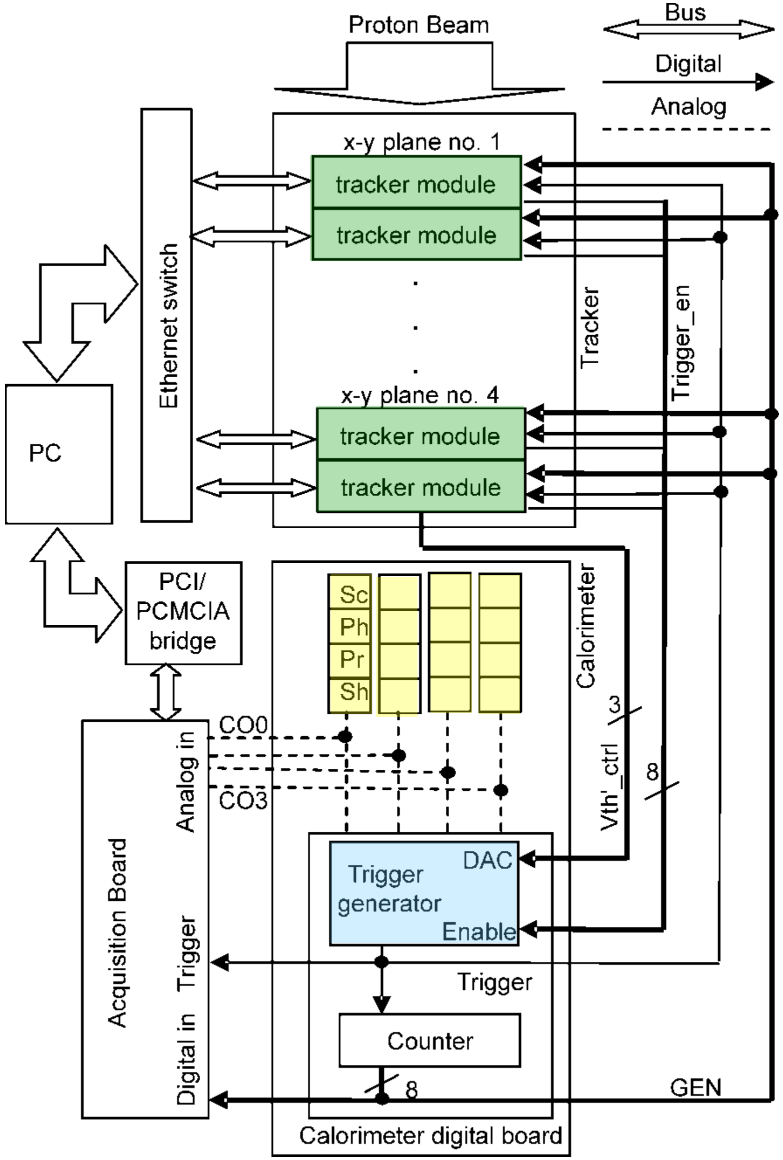

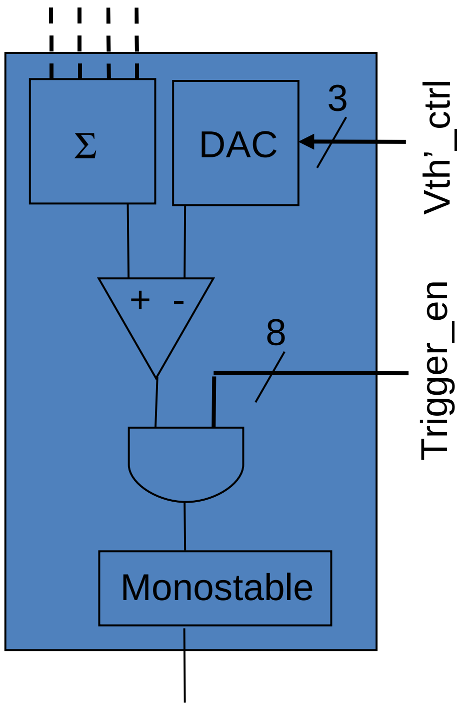

PRELIMINARY SINGLE CRYSTAL TEST (62MeV protons at LNS)

Charge spectra (62 MeV protons)

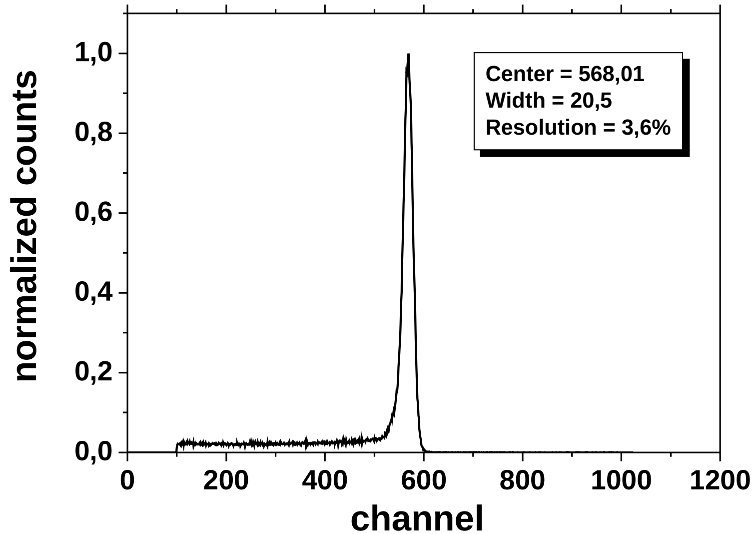

Cylindrical crystal, 2.5cm diameter.
Readout:pre-amp. CREMAT CR100, shaper Ortec 572

YAG:Ce properties	
Physical properties	
Density [g/cm³]	4.57
Hygroscopic0	0No
Chemical formula	$Y_3Al_5O_{12}$
Luminescence properties	
Wavelength of max. emission [nm]	550
Decay constant [ns]	70
Photon yield at 300k [10³ Ph/MeV]	40-50

Peak position vs beam energy

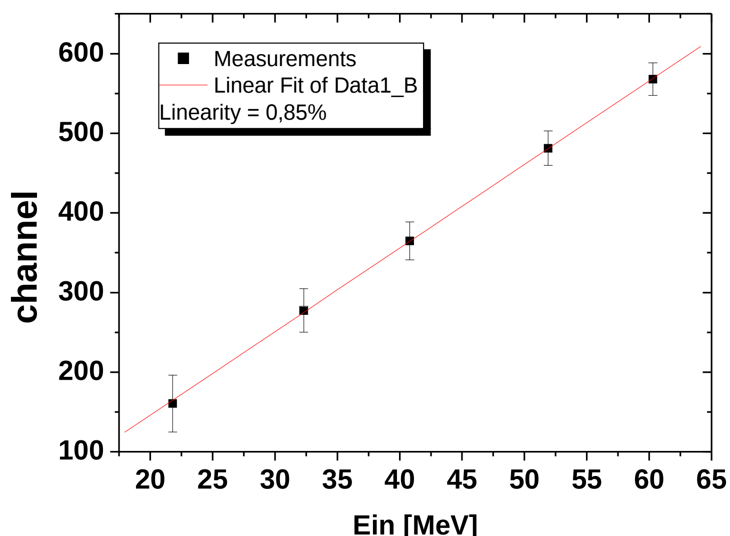

Resolution vs beam energy

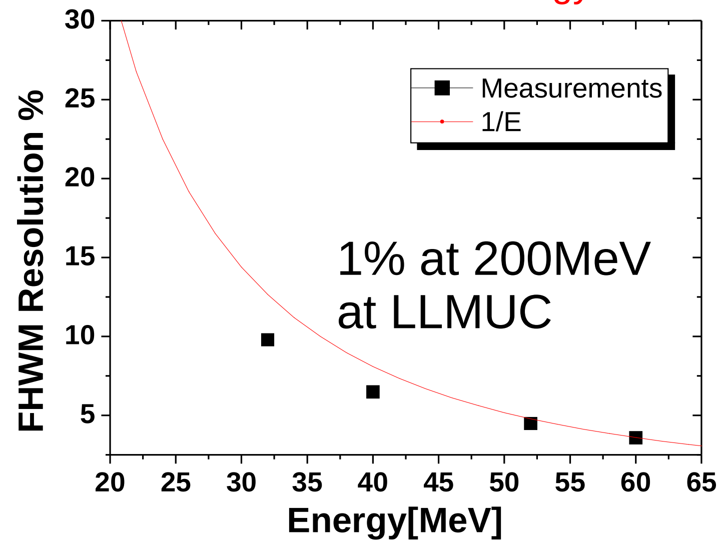

SEGMENTED CALORIMETER

Scintillator:

YAG:Ce optically separated crystals (Crytur),

0x30x100 mm^3 each.

eadout: 4 photodiodes (18x18 mm^2, Hamamatsu)

Different response of 4 crystals

(20% response variations, to be compensated with calibration).

Measured with 30-200MeV protons at LLMUC

Same resolution.

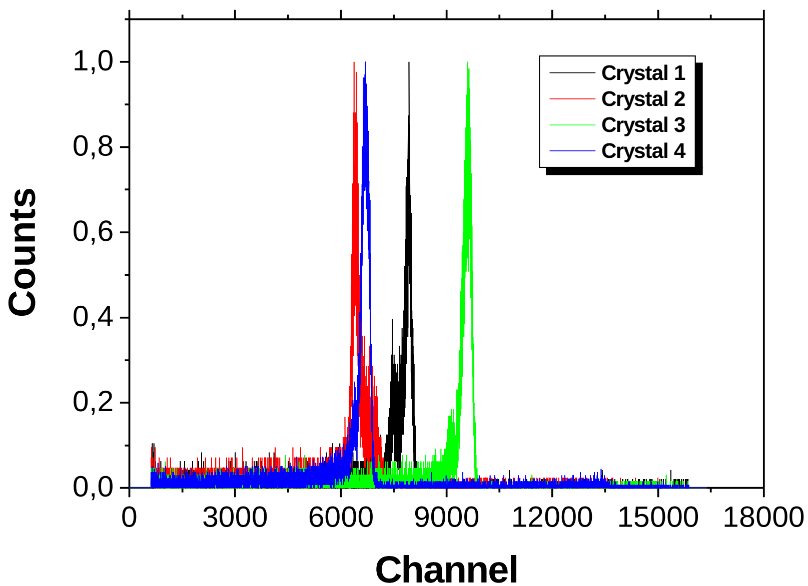

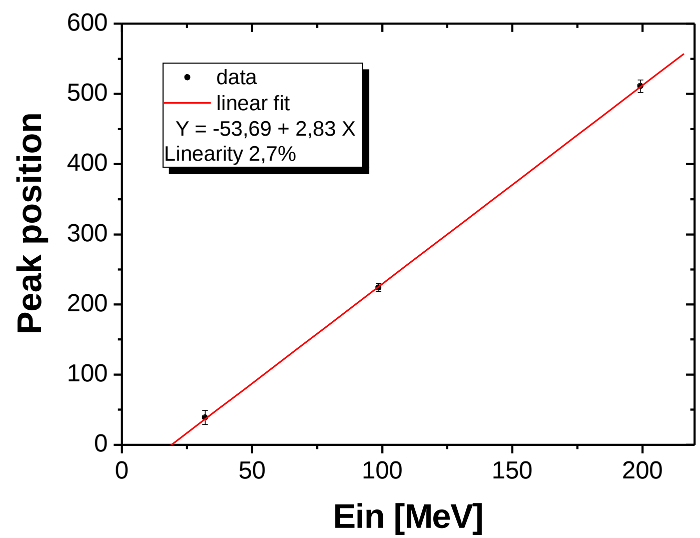

SINGLE CRYSTAL TEST (200 MeV protons at LLMUC)

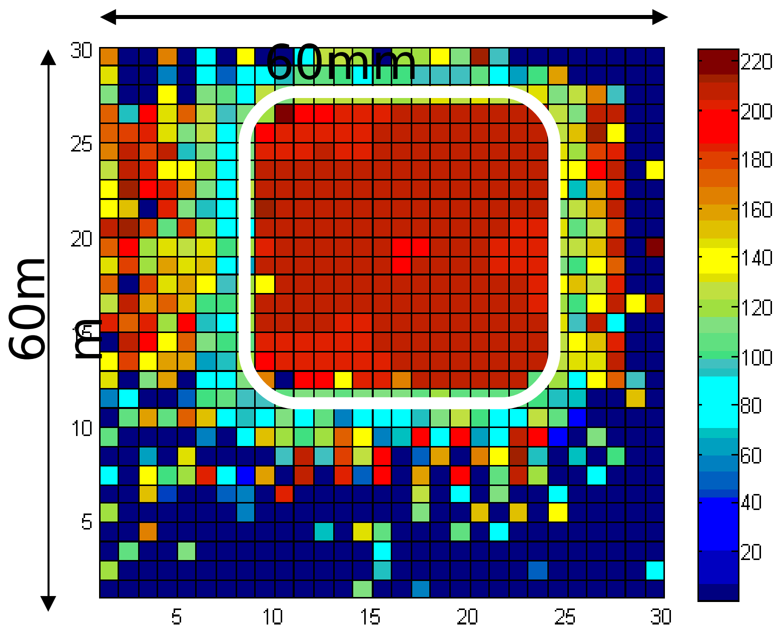

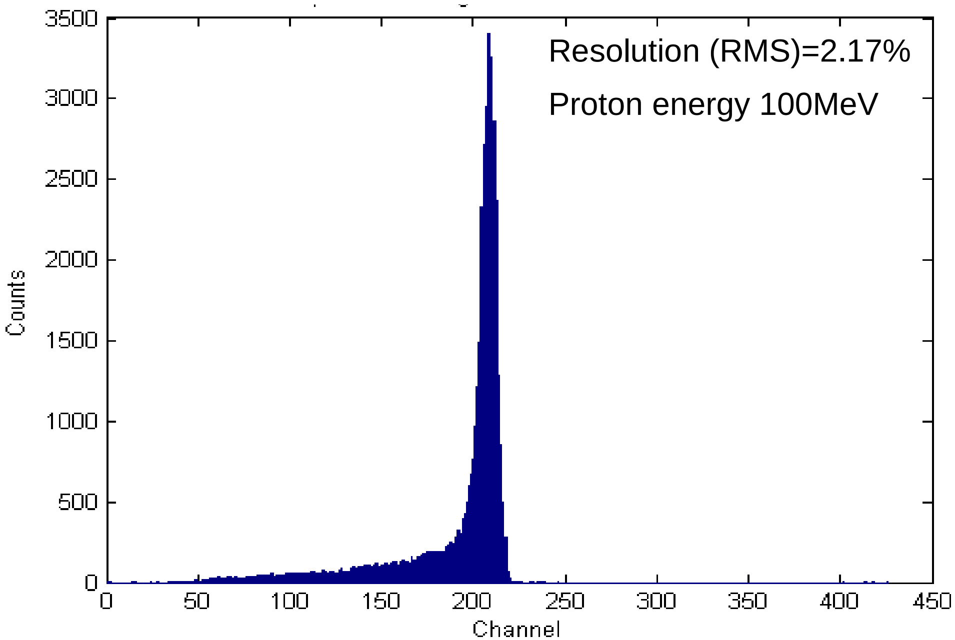

Homogeneity study

The tracker area (60X60mm^2) has been divided into 30x30 squares (2x2mm^2). For each square the charge spectrum has been made. This is the map of the charge spectrum peak position. Uniformity is ~1%.

Resolution

Charge spectrum of a crystal

Proton rate = 800 protons/sec

Area selected = 10 x 10 mm^2 (crystal center)

TRACKER MODULE- design

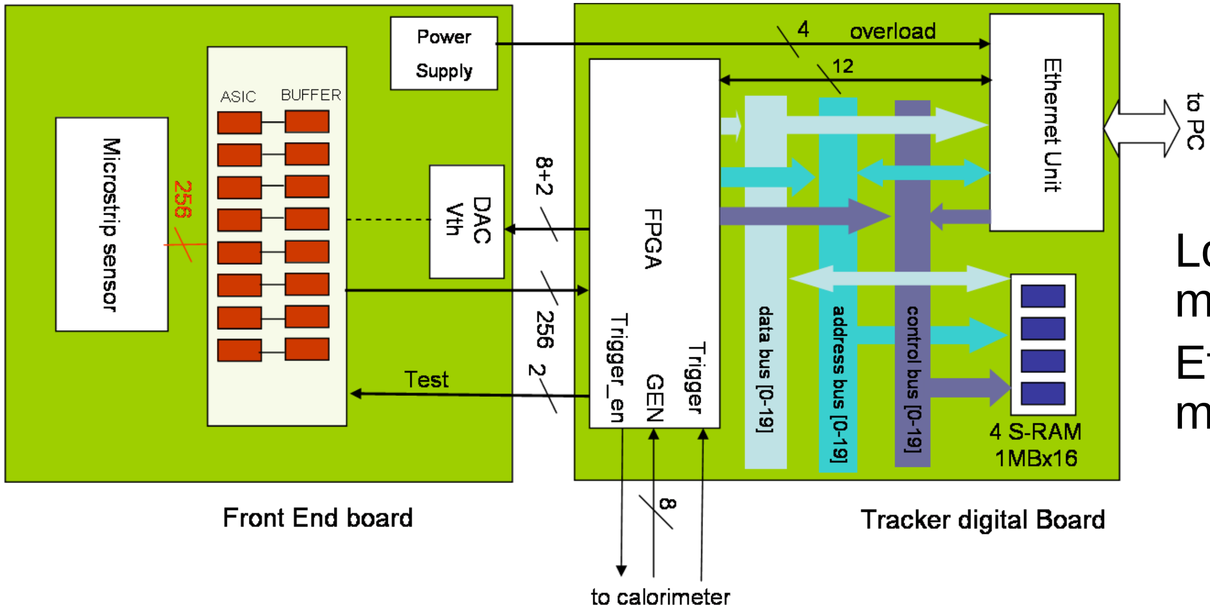

Local data storaging during measurement.

Ethernet data download at measurement completion.

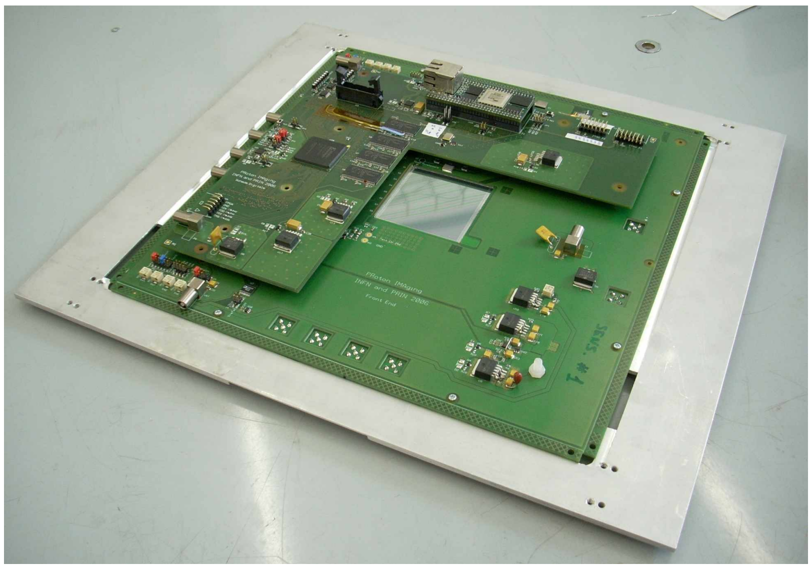

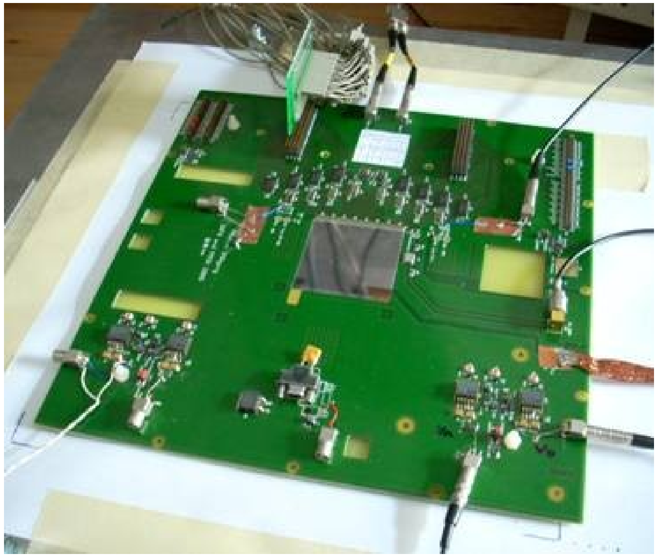

Si SENSOR

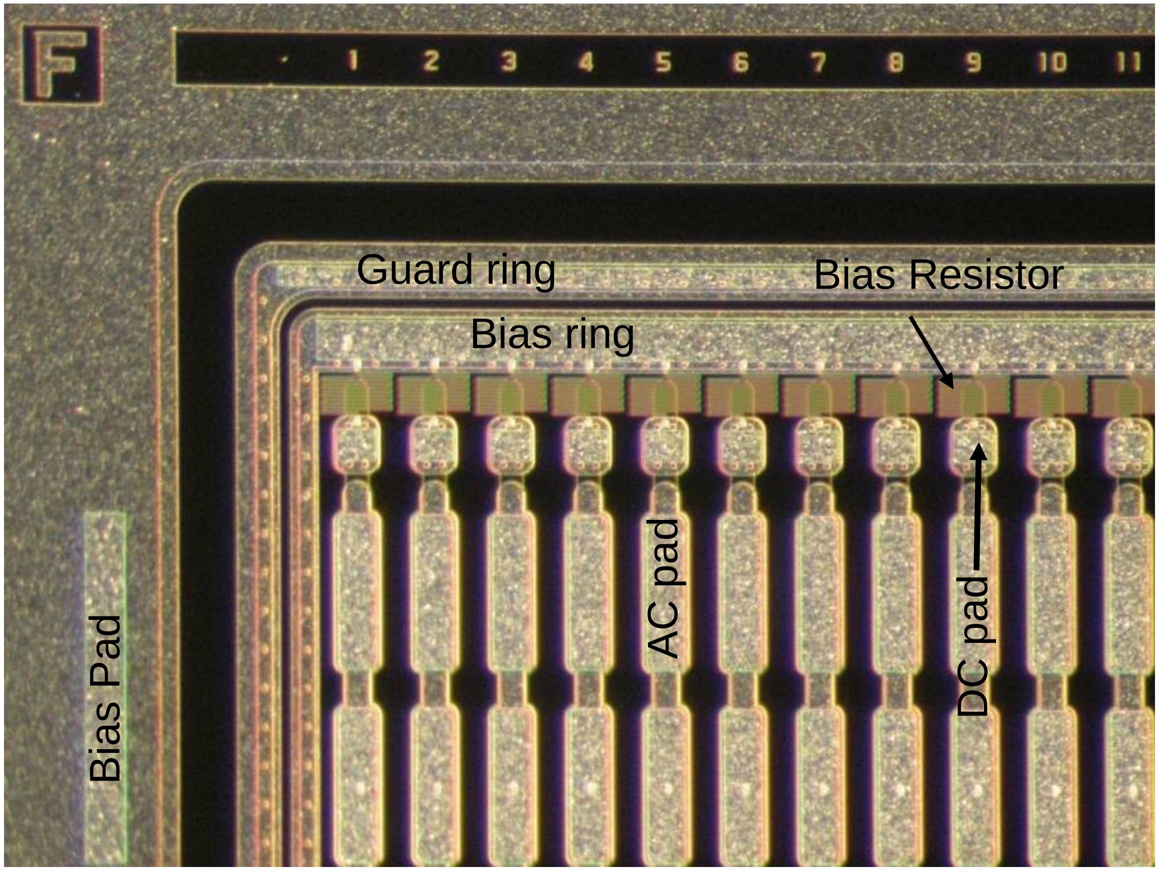

Manufactured by Hamamatsu Photonics

53x53 mm^2

p+-on-n strips

256 ch, 200 μm pitch

200 μm thickness
(To reduce the multiple scattering in the detector planes while keeping a good sensitivity to protons)

Proton Energy (MeV)	Energy Loss (keV/μm)	Released Energy (MeV)
10	9	1.8
30	3.5	0.7
50	2.5	0.5
100	1.4	0.28
200	0.8	0.16

BARE Si SENSOR PERFORMANCES

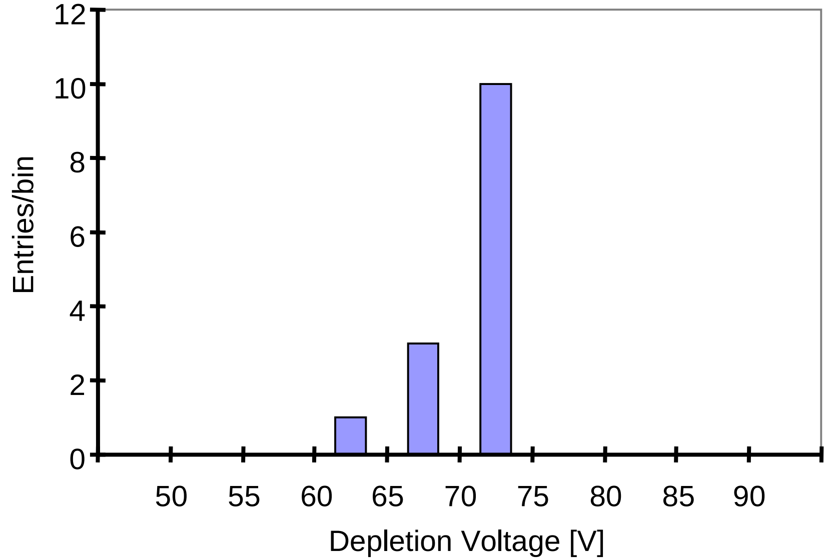

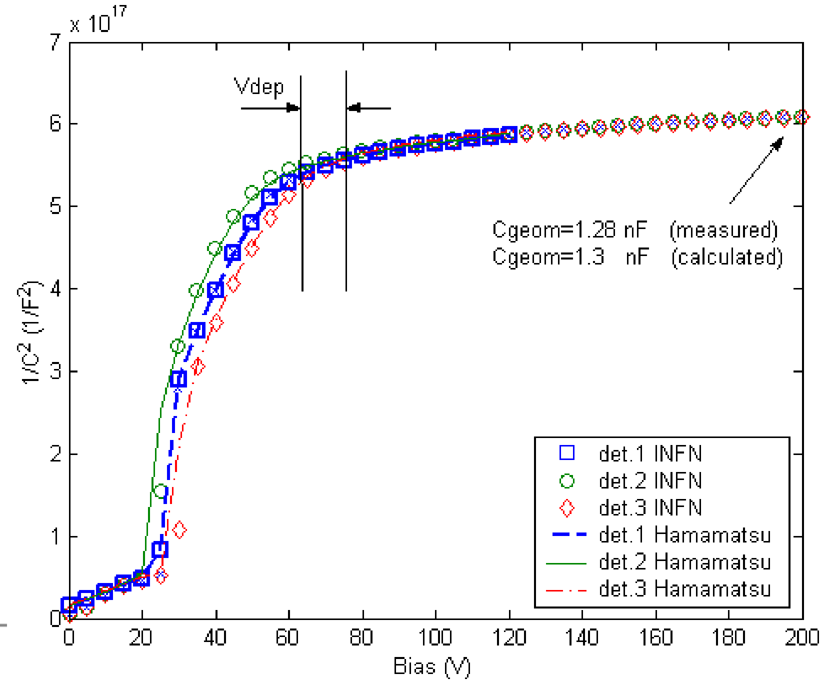

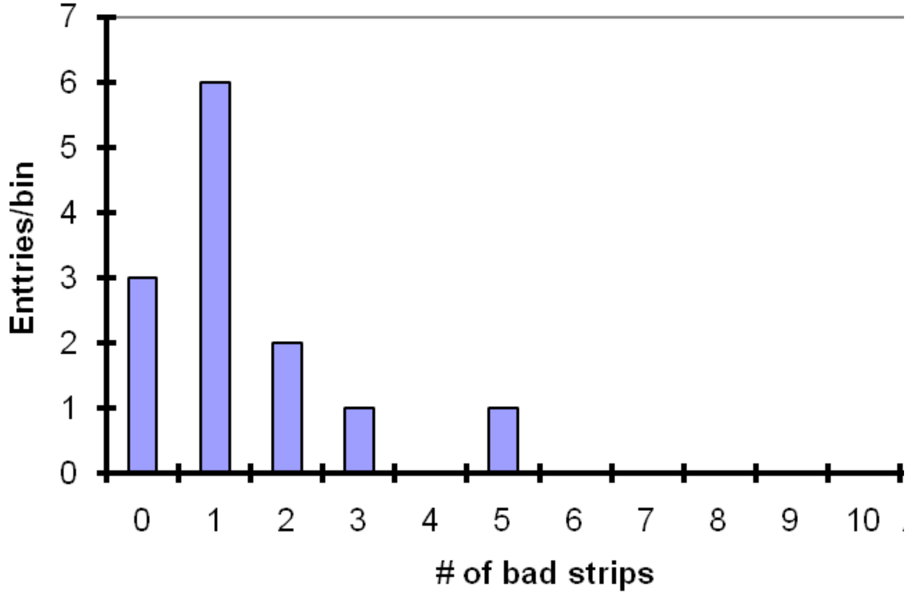

On a batch of 14 detectors:

V_{dep}<75 V (full depletion voltage)

i(100V)<1 μA

i(200V)<3 μA

C_{AC}= 54pF/cm (coupling capacitance)

C_{int}= 1.5 pF/cm (interstrip capacitance)

ASIC design

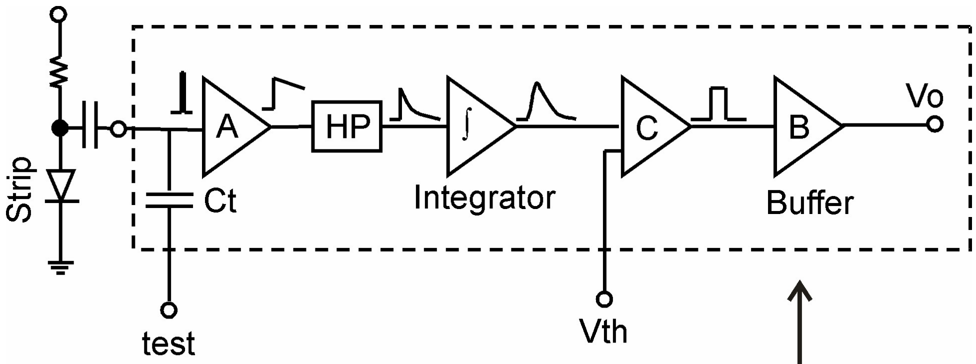

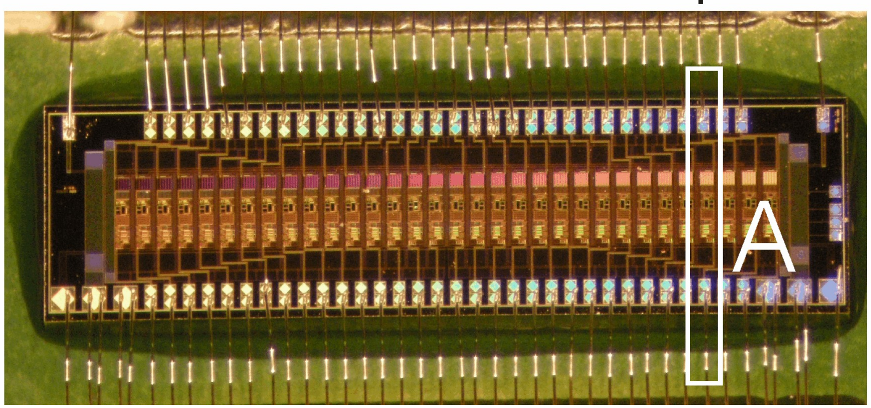

6.6 x 1.6 mm^2
32 inputs - 32 outputs
14.5mW/channel, 460 mW/chip power consumption
Vcc=+3.3 V
Channels uniformity: 2.5%

Output pad

Vda,Vdd, GND

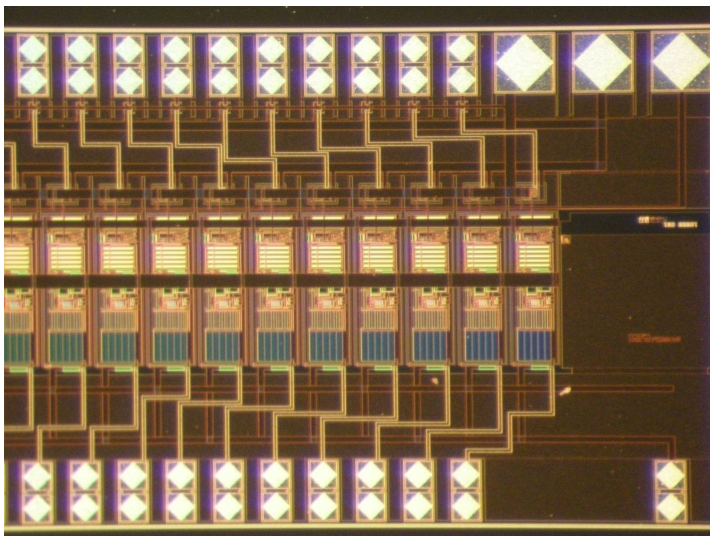

Input pad

Test

TRACKER FRONT END BOARD TEST: Calibration

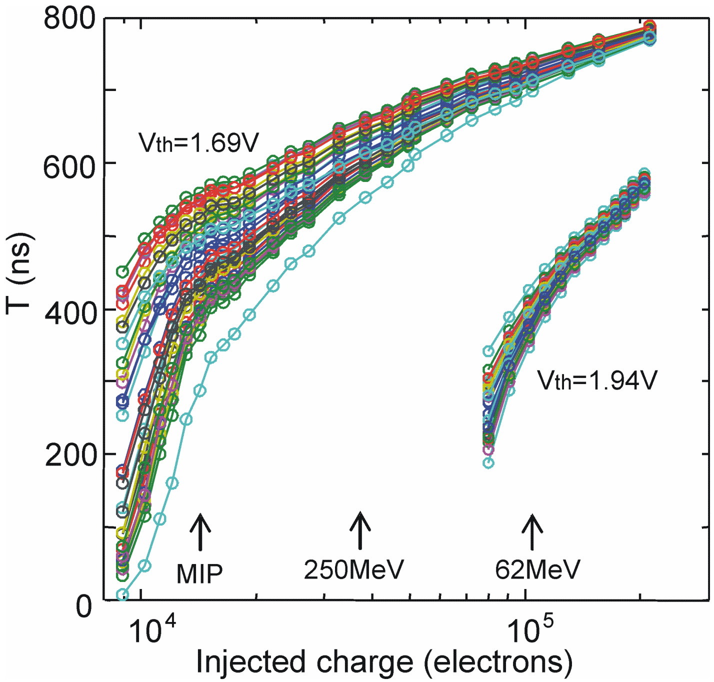

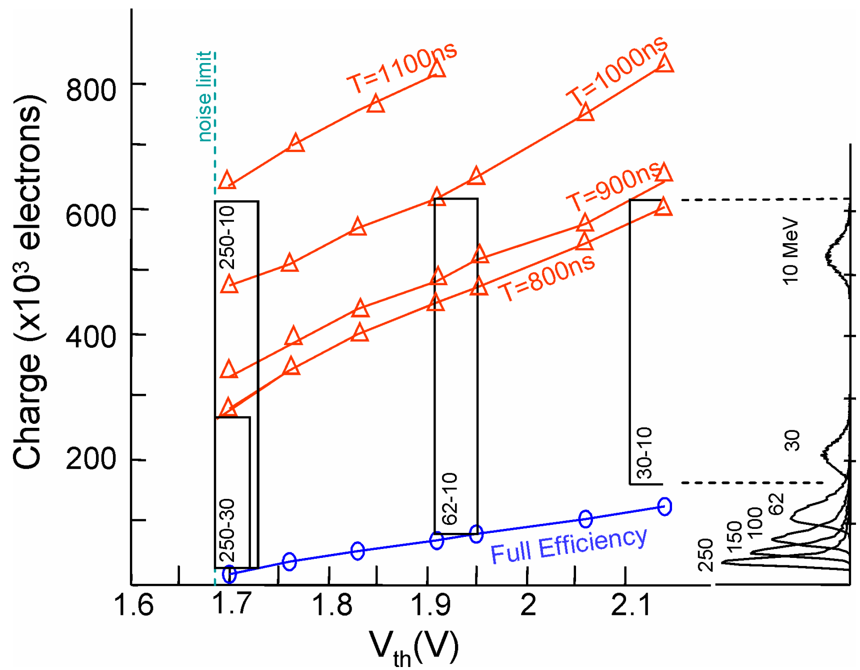

All channels read-out by tracker digital board.

a) No problems expected with tracking.

b) V_{th} coarse regulation board-by-board. Fine regulation chip-by-chip.

c) Possible difficulties with to energy loss measurements due to nonlinear chip response.

200 mm thick Si	Eloss MLK (MeV)	Q MLK (ke-)	Qmin (ke-)
MIP	0.052	16	~12
62 MeV protons	0.35	106	81
250 MeV protons	0.12	37	27

D. Menichelli et al., 2008 IEEE Nuclear Science Symposium Conference Record, 19-25 Oct. 2008, pp. 5600-608; IEEE Trans. Nucl. Sci., in press.

TRACKER FRONT END BOARD TEST: noise & efficiency

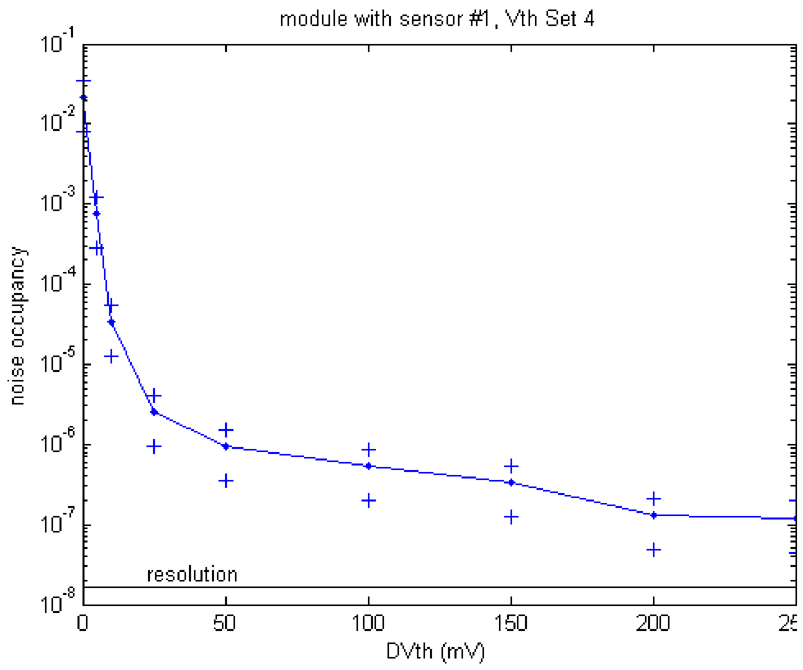

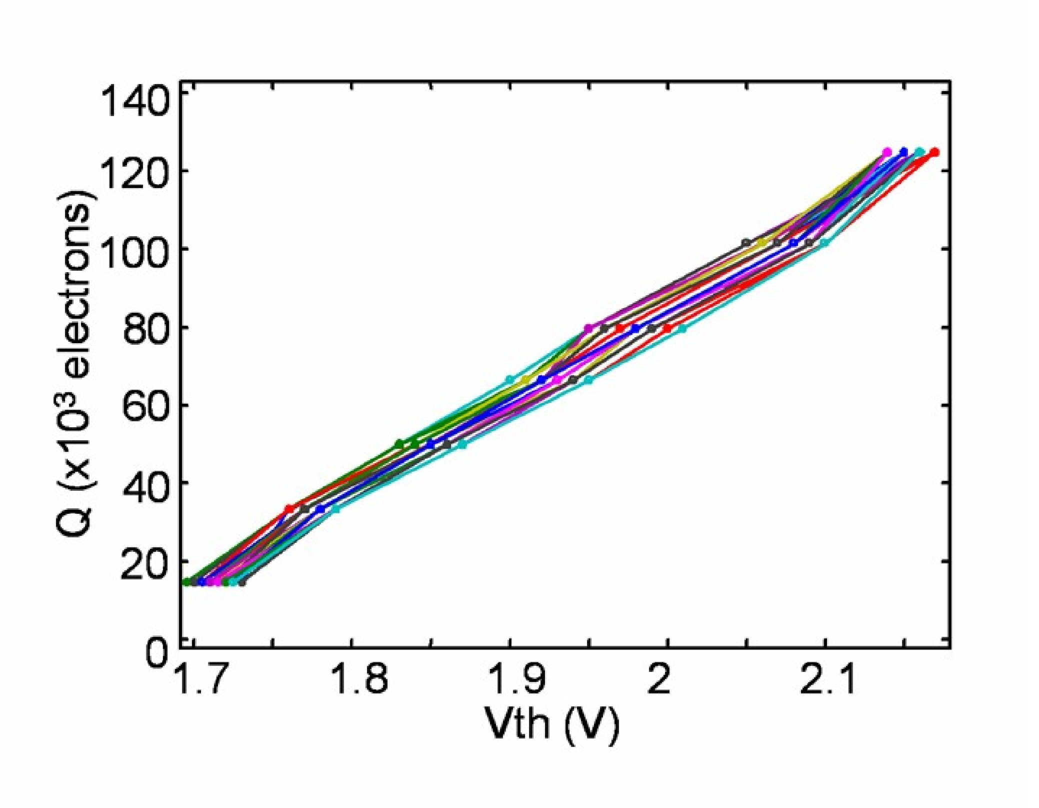

FRONT-END BOARD TEST: β

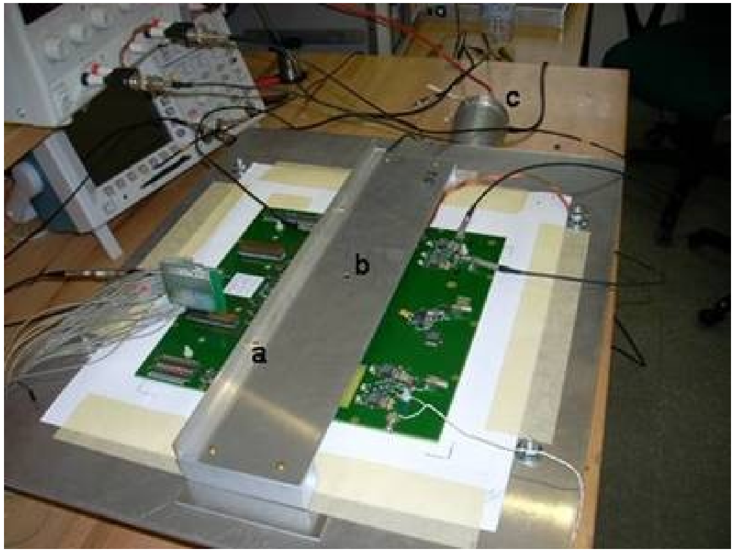

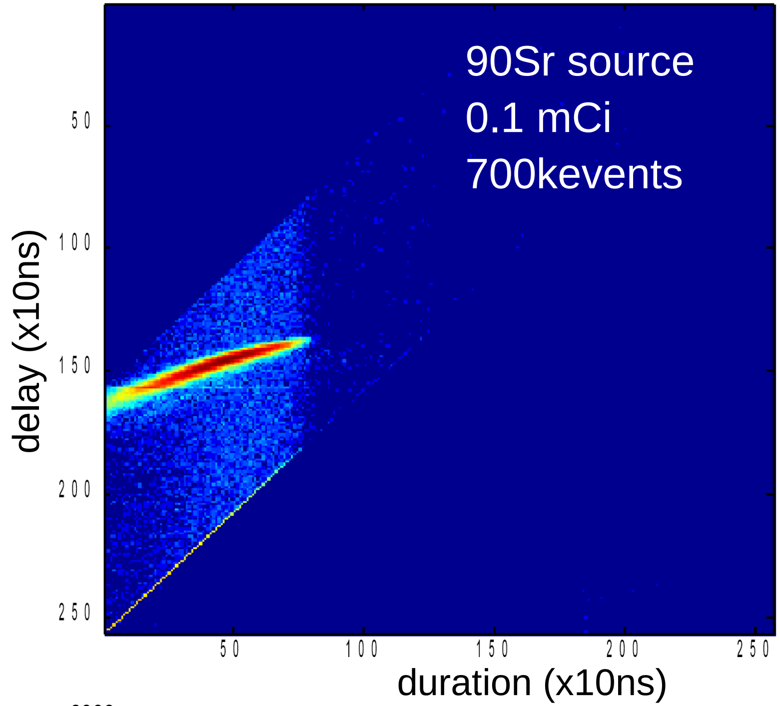

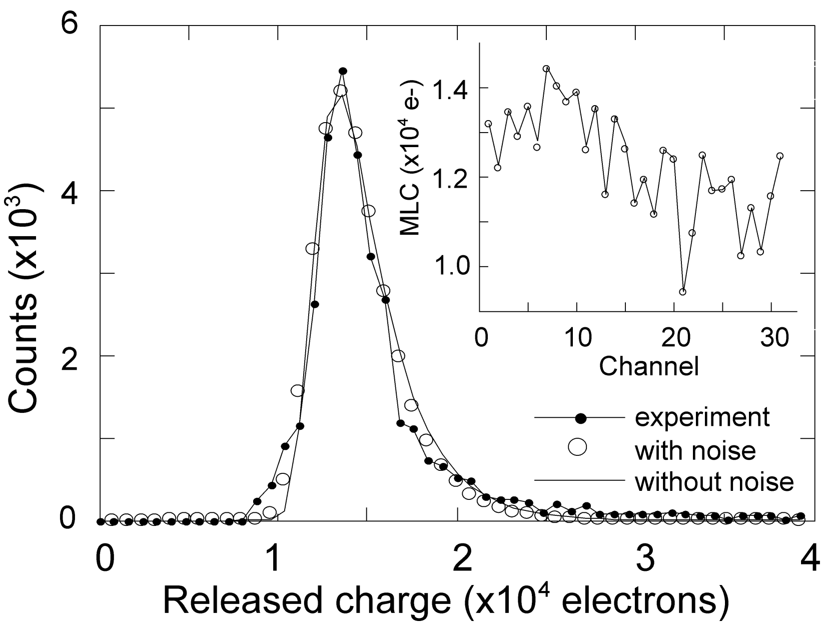

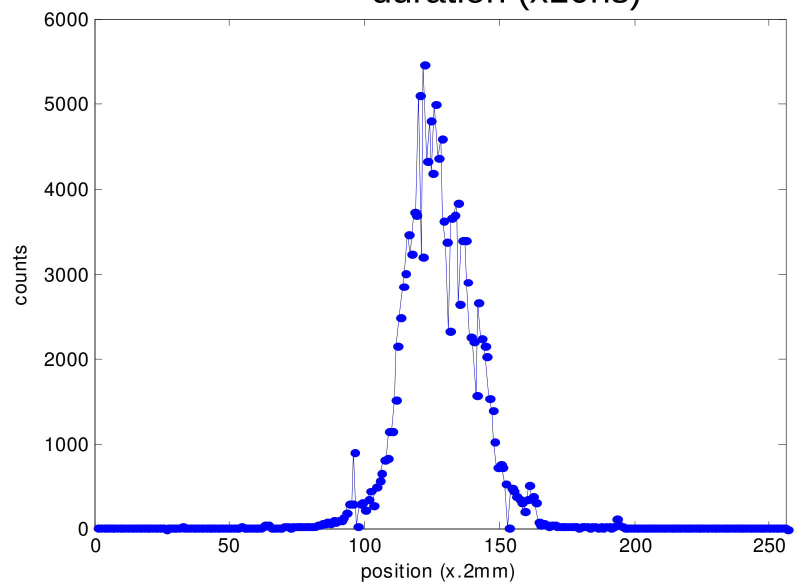

FRONT-END BOARD TEST: 62MeV PROTONS

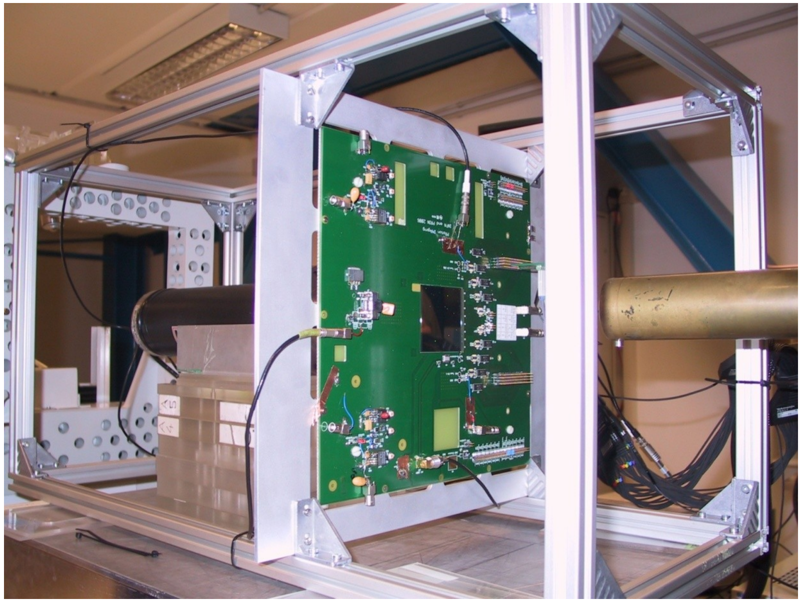

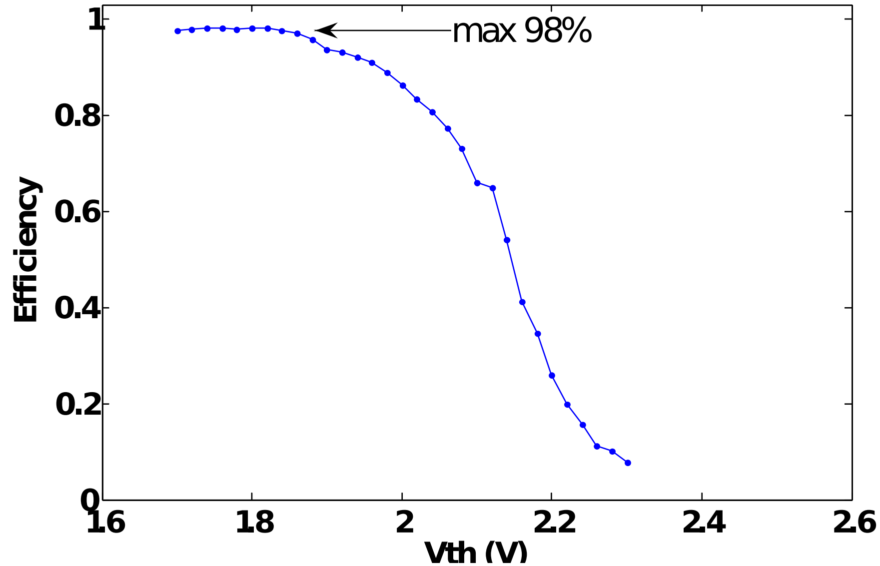

Efficiency remains at 98% for about 150mV above the noise limit.

The maximum values of the signal duration distributions are always well below 1μs. Further, measurements show that full efficiency, together with a signal duration less than 800ns, can be obtained for proton energies in the 30-250MeV range. This fact is very important to achieve a particle rate of 1MHz.

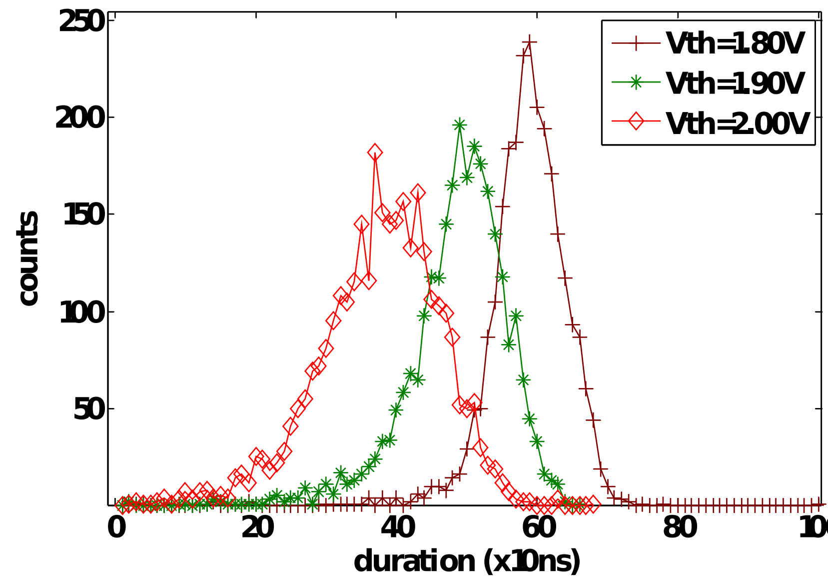

FRONT-END BOARD TEST WITH 62MeV PROTONS

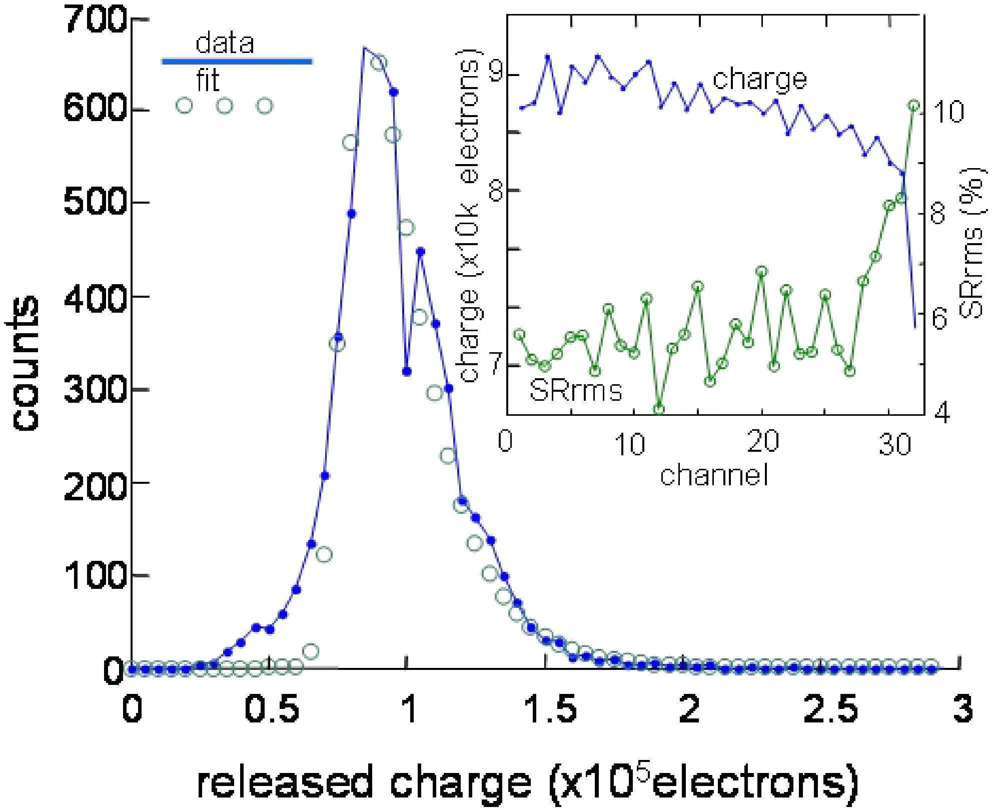

Typical charge spectrum measured with 62 MeV protons, obtained with $16\cdot10^3$ events and V_{th}=1.94V in the case of a single channel superimposed to a Landau fit. Most likely charge obtained by the fit for all the channels of a single ASIC is shown in the inset. Mean value is $87\cdot10^3$e; discrepancy with Monte Carlo predictions (105×10^3e) can be ascribed to the tolerance of integrated ASIC input capacitances.

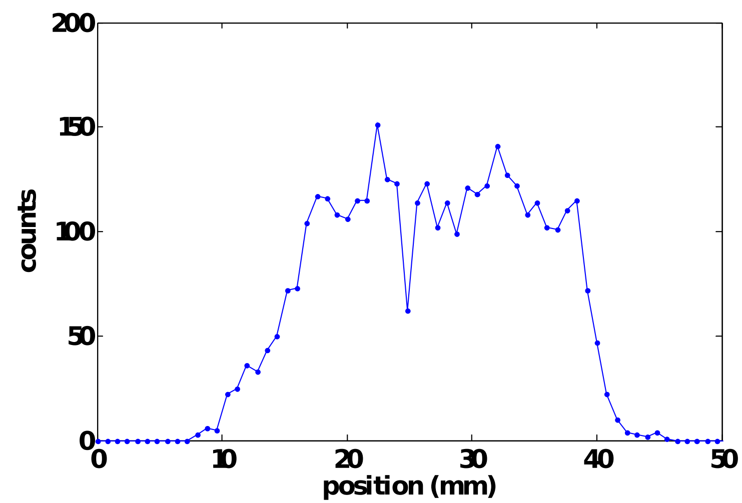

Beam profile. It reproduces fairly well the shape of the scintillator. The plot is not smooth due to the low statistics (about 4k events).

FUTURE PLANS (next 3 years)

End of 2009

Assembling of first xy plane and coupling with the calorimeter.

Tests with protons (a first beam test at LNS has been scheduled in October)

End of 2010

Complete integration of pCR telescope and first tests

Develoment of fast readout for the calorimeter

pCR test beams with protons: 62 MeV LNS + 200 MeV Essen WPC

Monte Carlo simulation of pCR device and analysis of experimental data.

End of 2011

R&D on possible improvements of the pCR apparatus

-detector upgrade (double side Si microstrip, other …) and scale-up

-new front end ASIC

-real time digital electronics (VIRTEX 5, other with embedded ethernet)

Further test beams with protons and data analysis

Development of reconstruction algorithms

End of 2012

pCT finalization with upgraded system

Development of real time data acquisition

Image reconstruction of pCT

References

D. Menichelli et al., "Characterization of a silicon strip detector and a YaG:Ce calorimeter for a proton computed radiography apparatus," IEEE Trans. Nucl. Sci., in press.

V. Sipala et al., Nucl. Inst. and Meth. A, in press. DOI:10.1016/j.nima.2009.08.029.

C. Talamonti et al., "Proton Radiography for Clinical Applications," Nucl. Instr. and Meth. A, in press. DOI:10.1016/j.nima.2009.08.040.

D. Menichelli et al., "Development of a Proton Computed Radiography Apparatus," 2008 IEEE Nucl. Science Symposium proceedings, 19-25 Oct. 2008, pp.1410-1415. DOI 10.1109 /NSSMIC.2008.4774679.

G. A. P. Cirrone et al., "Monte Carlo Studies of a Proton Computed Tomography System," IEEE Trans. Nucl. Sci., vol. 54, no. 5, October 2007, pp. 1487-1491.

M. Bruzzi et al., “Prototype Tracking Studies for Proton CT,” IEEE Trans. Nucl. Sci., vol. 54, no. 1, 2007, pp.140 - 145.

G.A.P. Cirrone et al., "The Italian project for a proton imaging device," Nucl. Instr. and Meth. A, vol. 576, no. 1, 11 June 2007, pp. 194-197.

G. Cuttone et al., "Detailed Monte Carlo Investigation of a proton Computed Tomography System," 2005 IEEE Nuclear Science Symposium Conference Record, 2873-2875.